

# Conflict Detection in AI-RAN: Efficient Interaction Learning and Autonomous Graph Reconstruction

Joao F. Santos\*, Arshia Zolghadr\*, Scott Kuzdeba†, and Jacek Kibilda\*

\*Commonwealth Cyber Initiative, Virginia Tech, USA, e-mail: {joaosantos, arshiaz, jkibilda}@vt.edu

†BAE Systems, Inc, e-mail: scott.kuzdeba@baesystems.us

**Abstract**—Artificial Intelligence (AI)-native mobile networks represent a fundamental step toward 6G, where learning, inference, and decision making are embedded into the Radio Access Network (RAN) itself. In such networks, multiple AI agents optimize the network to achieve distinct and often competing objectives. As such, conflicts become inevitable and have the potential to degrade performance, cause instability, and disrupt service. Current approaches for conflict detection rely on conflict graphs created based on relationships between AI agents, parameters, and Key Performance Indicators (KPIs). Existing works often rely on complex and computationally expensive Graph Neural Networks (GNNs) and depend on manually chosen thresholds to create conflict graphs. In this work, we present the first systematic framework for conflict detection in AI-native mobile networks, propose a two-tower encoder architecture for learning interactions based on data from the RAN, and introduce a data-driven sparsity-based mechanism for autonomously reconstructing conflict graphs without manual fine-tuning.

**Index Terms**—Mobile Networks, O-RAN, AI-RAN, Conflict Detection, Two-tower Encoder

## I. INTRODUCTION

One of the major developments toward 6G is the shift toward Artificial Intelligence (AI)-native mobile networks, where learning, inference, and decision-making are no longer treated as external add-ons, but are instead integrated into the network architecture itself [1]. Rather than relying on static, manually configured policies, the Radio Access Network (RAN) autonomously learns from data, makes real-time control decisions, and continuously adapts to network conditions, e.g., traffic demand, user mobility, and channel state. Such autonomy is achieved through a collection of intelligent controllers, e.g., dApps, xApps, and rApps in the context of O-RAN [2], or more broadly, through AI agents that perform learning-enabled control loops for optimizing the network to cater to diverse use cases and applications [1].

As multiple AI agents operate concurrently on the mobile network infrastructure, they may attempt to execute actions to achieve distinct or even conflicting objectives. For example, an agent may attempt to increase the transmit power to maximize throughput, while another agent simultaneously attempts to decrease the transmit power to minimize energy consumption [3]. This constitutes a *direct conflict*, which can degrade performance, cause instability, or disrupt service [3]. Other types of conflicts also exist, including *indirect* and *implicit* conflicts. For examples, differences between types of conflicts and formal definitions, we refer the reader to [4], [5]. Despite the potential vulnerabilities introduced by conflicting control decisions in AI-native mobile networks, research on conflict

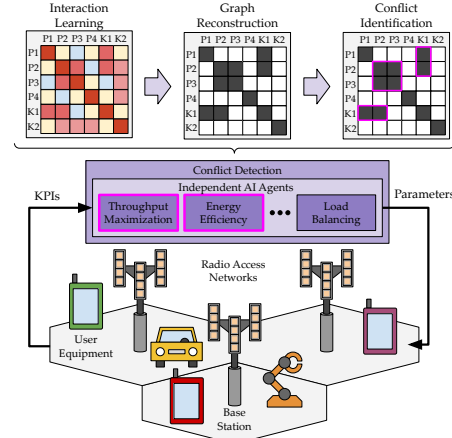


Fig. 1: Our proposed conflict detection framework for AI-native mobile networks, where independent AI agents control the RAN to achieve distinct and possibly conflicting objectives.

detection and mitigation remains in its early stages.

In the literature to date, works on conflict detection represent the relationships between AI agents, the RAN parameters they control, and Key Performance Indicators (KPIs) they subscribe to as graphs [3], [5], [6], and detect conflicts by analyzing the topology of these graphs [3]. The first challenge is inferring the graph topology from data collected from the RAN, which is achieved by learning interactions between agents, parameters, and KPIs. To date, autonomous methods such as Graph Neural Networks (GNNs) have been proposed [5], at the cost of complex and computationally expensive message-passing operations [7]. Once interactions are learned, an appropriate decision rule must be applied to determine which interactions are meaningful and constitute relationships to create the graph topology. Here, existing works rely on manually selected thresholds to identify relevant interactions [3], [8], an approach that is difficult to generalize across datasets and deployment scenarios. While existing works address different aspects of the conflict detection problem, there is a lack of a systematic framework to characterize their design choices and trade-offs.

In this work, we address these open challenges by first framing conflict detection in AI-native mobile networks as a three-stage problem comprising (i) interaction learning, (ii) graph reconstruction, and (iii) conflict identification, as shown in Fig. 1. Next, we posit interaction learning as a ranking problem, often encountered in recommender systems [9], and propose a lightweight two-tower encoder architecture

for efficiently learning interactions from data collected from the RAN [10]. Then, we develop a data-driven, sparsity-based mechanism that autonomously selects relevant interactions [11], enabling conflict graph reconstruction without manual fine-tuning across datasets and scenarios. Finally, we evaluate our conflict detection solution using the rule-based conflict identification approach proposed in [5].

The main contributions of this paper are as follows:

- We propose a framework for decomposing conflict detection as a three-stage problem comprised of (i) interaction learning, (ii) graph reconstruction, and (iii) conflict identification.
- We model the interaction learning stage as a ranking problem between parameters and KPIs, and propose a two-tower encoder architecture for efficiently learning interactions.
- We introduce a data-driven, sparsity-based approach for selecting relevant interactions, enabling autonomous graph reconstruction without the need for manual fine-tuning.
- We validate the efficiency of our proposed conflict detection solution using a dataset of Gaussian-distributed parameters and KPIs generated from a known conflict model [12].

In the following sections, we present our systematic framework for conflict detection, and assess related works with respect to their design choices. Next, we introduce our proposed solutions for efficient interaction learning and autonomous graph reconstruction, and compare their performance against existing solutions. Finally, we make our concluding remarks.

## II. THE THREE STAGES OF CONFLICT DETECTION

The existing literature on conflict detection in AI-native mobile networks commonly adopts a graph-based model [3], [6], [8] to represent AI agents, RAN parameters, and KPIs as nodes, and their relationships as edges, forming a conflict graph  $\mathcal{G} = (\mathcal{V}, \mathcal{E})$ . We can denote the set of independent AI agents as  $\mathcal{A}$ , the set of RAN parameters as  $\mathcal{P}$ , and the set of KPIs as  $\mathcal{K}$ , and define the set of vertices  $\mathcal{V} = \mathcal{A} \cup \mathcal{P} \cup \mathcal{K}$ , while the set of edges  $\mathcal{E}$  describes the relationships (or lack thereof) between these entities. In this graph, an edge between (i) an agent  $a \in \mathcal{A}$  and a parameter  $p \in \mathcal{P}$  represents that the agent controls the parameter, (ii) a parameter  $p \in \mathcal{P}$  and a KPI  $k \in \mathcal{K}$  represents that the parameter influences the KPI, and (iii) a KPI  $k \in \mathcal{K}$  and an agent  $a \in \mathcal{A}$  represents that the value of the KPI informs the agent's decision. This modeling approach enables the identification and categorization of conflicts through the analysis of the graph structure, represented by an adjacency matrix  $\mathbf{A}$ .

The relationships between agents and the parameters they control, as well as the KPIs they observe to make decisions, are often explicit and known by design, since agents must request access to the network infrastructure for modifying control parameters and accessing KPIs [2]. In contrast, the relationships between parameters and KPIs are often non-trivial and dynamic, emerging over time or manifesting under specific operating conditions [5], [6]. When combined with interdependencies among parameters themselves, and among KPIs, these relationships can form complex chains of dependencies that are difficult to identify in advance. As a result, the major challenge for conflict detection in AI-native mobile networks lies in learning relationships between parameters and

KPIs, while also capturing relationships within each of these entities, based on data collected from the RAN. This problem can be decomposed into three stages.

To formalize this decomposition, we consider datasets of samples collected from the RAN, e.g., from simulations or real-world observations. Let  $\mathbf{X}_p \in \mathbb{R}^{N_p \times L}$  denote  $L$  samples of  $N_p = |\mathcal{P}|$  parameters, and  $\mathbf{X}_k \in \mathbb{R}^{N_k \times L}$  denote  $L$  samples of  $N_k = |\mathcal{K}|$  KPIs. While, a binary matrix  $\mathbf{A}_{\text{known}} \in \{0, 1\}^{N_a \times (N_p + N_k)}$  encodes the known relationships between the  $N_a = |\mathcal{A}|$  agents with parameters and KPIs based on the information obtained from the RAN control plane (in the case of O-RAN, these would be obtained through the Subscription Manager [2]). An element  $[\mathbf{A}_{\text{known}}]_{i,j} = 1$  indicates agent  $i$  controls (or subscribes) to parameter (or KPI)  $j$ , and  $[\mathbf{A}_{\text{known}}]_{i,j} = 0$  indicates otherwise. Then, we define the following three stages of conflict detection:

- **Stage I – Interaction Learning:** This stage focuses on *learning interactions* between parameters and KPIs from data collected from the RAN. Given  $\mathbf{X}_p$  and  $\mathbf{X}_k$ , a reconstruction approach assigns *scores* capturing the strength or relevance of their interactions:

$$\mathbf{S} = \mathcal{R}(\mathbf{X}_p, \mathbf{X}_k) = \begin{bmatrix} \mathbf{S}_{pp} & \mathbf{S}_{pk} \\ \mathbf{S}_{kp} & \mathbf{S}_{kk} \end{bmatrix}, \quad \mathbf{S}_{kp} = \mathbf{S}_{pk}^\top, \quad (1)$$

where  $\mathcal{R}(\cdot)$  denotes the learning method, e.g., statistical profiling, causal inference, or GNNs. The type of score depends on the chosen learning method, e.g., Kolmogorov-Smirnov distance [3], correlation [5], or similarity. The resulting score matrix  $\mathbf{S} \in \mathbb{R}^{(N_p + N_k) \times (N_p + N_k)}$  captures cross-entity interactions between parameters and KPIs ( $\mathbf{S}_{pk} \in \mathbb{R}^{N_p \times N_k}$ ), as well as same-entity interactions among parameters ( $\mathbf{S}_{pp} \in \mathbb{R}^{N_p \times N_p}$ ) and among KPIs ( $\mathbf{S}_{kk} \in \mathbb{R}^{N_k \times N_k}$ ).

- **Stage II – Graph Reconstruction:** The second stage focuses on *re-creating conflict graphs* from learned scores and known relationships from agents. Given  $\mathbf{S}$ , a binarization approach determines the relevant interactions and maps the real-valued scores into a partial adjacency matrix:

$$\hat{\mathbf{A}}_{\text{learned}} = \mathcal{B}(\mathbf{S}), \quad (2)$$

where  $\mathcal{B}(\cdot)$  denotes the score binarization method, e.g., thresholds [3], sparsity, or other strategies.  $\hat{\mathbf{A}}_{\text{learned}} \in \{0, 1\}^{(N_p + N_k) \times (N_p + N_k)}$  encodes topological information describing relationships between parameters and KPIs, as well as among parameters, and among KPIs. We augment  $\hat{\mathbf{A}}_{\text{learned}}$  with  $\mathbf{A}_{\text{known}}$  to generate the adjacency matrix [3]:

$$\hat{\mathbf{A}} = \hat{\mathbf{A}}_{\text{learned}} \boxplus \mathbf{A}_{\text{known}} = \begin{bmatrix} \mathbf{I}_{N_a} & \mathbf{A}_{\text{known}} \\ \mathbf{A}_{\text{known}}^\top & \hat{\mathbf{A}}_{\text{learned}} \end{bmatrix}, \quad (3)$$

where  $\boxplus$  denotes a block-wise matrix augmentation operation, adding  $\mathbf{A}_{\text{known}}$  as additional rows above  $\hat{\mathbf{A}}_{\text{learned}}$ , along with the corresponding  $\mathbf{A}_{\text{known}}^\top$  as additional columns before  $\hat{\mathbf{A}}_{\text{learned}}$  [3], and filling the remaining block corresponding to relationships among agents as an identity matrix  $\mathbf{I}_{N_a}$ . This operation yields a binary adjacency matrix  $\hat{\mathbf{A}} \in \{0, 1\}^{(N_a + N_p + N_k) \times (N_a + N_p + N_k)}$  that approximates  $\mathbf{A}$  and represents a conflict graph.

- **Stage III – Conflict Identification:** The final stage focuses on analyzing the graph topology to identify different types

of conflicts, i.e., direct, indirect, and implicit [4]. Given  $\hat{A}$ , an identification approach searches the conflict graph for subgraphs representing the different conflicts:

$$C = \mathcal{I}(\hat{A}), \quad (4)$$

where  $\mathcal{I}(\cdot)$  denotes the conflict identification method, e.g., rule-based [5], or exact graph isomorphism algorithms. The resulting set  $C$  contains the different types of identified conflicts between  $\mathcal{A}$ ,  $\mathcal{P}$  and  $\mathcal{K}$ .

We can now express the conflict detection problem as a combination of the three stages, as illustrated in Fig. 1:

$$C = \mathcal{I}(\mathcal{B}(\mathcal{R}(\mathbf{X}_p, \mathbf{X}_k)) \boxplus \mathbf{A}_{\text{known}}). \quad (5)$$

By decomposing conflict detection, we can focus on the design choices and trade-offs of individual stages, while also enabling better categorization of existing works.

### III. RELATED WORKS

The literature on conflict detection has primarily focused on O-RAN, where AI agents exist in the form of xApps and rApps, with explicit visibility into parameters and KPIs. Early works focused on rule-based approaches for detecting conflicts based on the performance degradation of KPIs [8], [13]. These approaches set operating ranges for KPI values and tracked parameter changes, characterizing conflicts as KPI deviations from these ranges and attributing their cause to the most recent parameter change. These works assume all relationships between agents, parameters, and KPIs are known in advance. As a result, they do not perform interaction learning or graph reconstruction and only apply a rule-based conflict identification. However, it is unclear how such relationships can be determined, nor how this approach could be applied to networks with different sets of agents, parameters, and KPIs.

To address this limitation, more recent works started learning interactions between parameters and KPIs to reconstruct conflict graphs. For example, the work of [3] generated statistical profiles of agents operating in a sandbox environment, akin to a digital twin, learning interactions between parameters and KPIs through Empirical Cumulative Distribution Functions (ECDFs), and determined the relevant interactions for creating conflict graphs using the Kolmogorov–Smirnov distance between the ECDFs, followed by a rule-based conflict identification. However, the effectiveness of the resulting conflict graph (and consequently conflict detection) relies on the choice of an arbitrary set of tests and the fidelity of the sandbox in capturing realistic network behavior.

Other works have addressed the reliance on arbitrary testing within digital twins by exploring data-driven techniques for learning how relationships between parameters and KPIs emerge from data collected from the RAN. For example, the work of [6] inferred cause and effect relationships between parameters and KPIs by adopting regression models for learning interactions between parameters and KPIs, and leveraging SHapley Additive exPlanations (SHAP) values with manually chosen thresholds to create asymmetric conflict graphs. This approach has the potential to enable root-cause analysis for tracing the origin of a conflict. However, it is limited to identifying indirect conflicts, as it does not consider

the relationships between agents with parameters and KPIs. Meanwhile, the work of [5], adopted a GNN for learning interactions between parameters and KPIs using correlation, and manually chosen thresholds to select relevant relationships to reconstruct conflict graphs, followed by a rule-based conflict identification. While this approach allows the identification of conflicts with high accuracy, GNNs are complex and computationally expensive, requiring combinatorial exploration of interactions through repeated message-passing operations [7].

In this work, we propose a lightweight approach for learning interactions between parameters and KPIs, and an autonomous approach for graph reconstructions. In the following two sections, we introduce (i) a two-tower encoder architecture inspired by the ranking problems encountered in recommender systems [9], that is simpler and more scalable than GNN-based solutions, and (ii) a sparsity-based approach for selecting relevant interactions [11], that is more general than existing threshold-based solutions and can reconstruct graphs without manual fine-tuning to specific datasets or scenarios.

### IV. PROPOSED INTERACTION LEARNING METHOD

To simplify training, reduce computational costs, and accelerate learning of interactions between parameters and KPIs, we propose a two-tower encoder architecture for interaction learning, as illustrated in Fig. 2. We adopt two independent encoders, known as towers, that project different types of input objects into a shared, lower-dimensional latent space, and then, we propose to calculate the relevance of their interactions using scaled dot-product similarity [10]. In the following, we detail the formulation of our two-tower encoder architecture, and describe how we can reconstruct the score matrix in (1).

#### A. Two-Tower Encoder Architecture

We define a two-tower encoder architecture that independently encodes  $\mathbf{X}_p$  and  $\mathbf{X}_k$  into a shared latent space of dimension  $H$ :

$$\mathbf{Z}_p = f_p(\mathbf{X}_p, \theta_p) \in \mathbb{R}^{N_p \times H}, \quad (6a)$$

$$\mathbf{Z}_k = f_k(\mathbf{X}_k, \theta_k) \in \mathbb{R}^{N_k \times H}, \quad (6b)$$

where  $f_p(\cdot)$  and  $f_k(\cdot)$  are learnable encoders,  $\theta_p$  and  $\theta_k$  denote the trainable weights of the parameter and KPI encoders, respectively, and  $\mathbf{Z}_p$  and  $\mathbf{Z}_k$  represent the node embeddings of parameters and KPIs in the latent space, respectively.

It is worth noting that our two-tower encoder architecture does not depend on a specific encoder architecture. The encoders can be realized using different models depending on the nature of the training data and the objective of the learning task. In our current realization, each encoder comprises a lightweight feed-forward network composed of a linear layer followed by a Rectified Linear Unit (ReLU) activation layer, and a final linear output layer, similar to [14], as illustrated in Fig. 2. Alternative models for the encoders may include, e.g., temporal models for capturing the dynamic evolution of the system [15]. We detail the training of our two-tower encoder architecture later in Section VI-A.

To quantify the strength of the interactions between parameters and KPIs in the latent space, we first apply a row-wise L2-normalization on the node embeddings to ensure they have

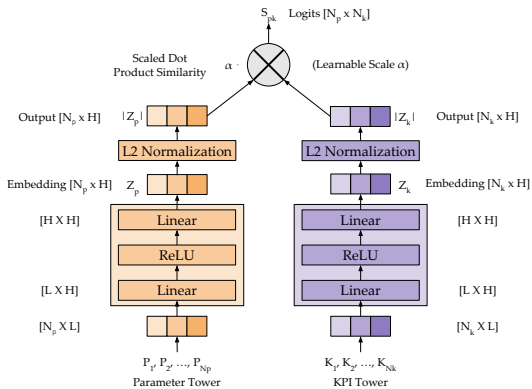


Fig. 2: Our two-tower encoder architecture, showing the operations for independently encoding parameters and KPI into the latent space. We calculate the similarity of their node embeddings to infer interactions between parameters and KPIs. comparable scales, and prevent the embedding magnitude from dominating the calculation of their similarity scores, i.e.:

$$||\mathbf{Z}_p||_{i,:} = \frac{[\mathbf{Z}_p]_{i,:}}{\|[\mathbf{Z}_p]_{i,:}\|_2}, \quad \forall i = 1, \dots, N_p, \quad (7a)$$

$$||\mathbf{Z}_k||_{j,:} = \frac{[\mathbf{Z}_k]_{j,:}}{\|[\mathbf{Z}_k]_{j,:}\|_2}, \quad \forall j = 1, \dots, N_k, \quad (7b)$$

where  $\|\cdot\|_2$  is the L2-norm operator,  $[\cdot]_{i,:}$  is the  $i$ -th row of a matrix  $\cdot$ , while  $|\cdot|$  denotes the normalized node embedding.

Finally, we apply a scaled dot-product similarity between  $|\mathbf{Z}_p|$  and  $|\mathbf{Z}_k|$  to quantify the strength of their interaction based on their alignment in the latent space:

$$S_{pk} = \alpha |\mathbf{Z}_p| |\mathbf{Z}_k|^T \in \mathbb{R}^{N_p \times N_k}, \quad (8)$$

where  $S_{pk}$  is a partial score matrix containing similarity values between parameters and KPIs, and  $\alpha \in \mathbb{R}_+$  is a learnable scale parameter for re-scaling the dot product similarity [9].

### B. Score Matrix Reconstruction

Once training is complete,  $S_{pk}$  enables the identification of *indirect* conflicts between parameters and KPIs. However, this partial matrix alone is insufficient for detecting *implicit* conflicts, which arise through complex chains of interactions involving multiple parameters, KPIs, and AI agents. Identifying such conflicts also require information about same-entity interactions among parameters and among KPIs, which are not directly observable from measurements of parameters and KPIs. To address this issue, we train our two-tower architecture to learn cross-entity interactions between parameters and KPIs, from (8), and subsequently leverage the learned node embeddings to infer same-entity interactions among parameters and among KPIs, and construct the score matrix in (1).

To accomplish this, first we concatenate the learned  $\mathbf{Z}_p$  and  $\mathbf{Z}_k$  after training to form a unified embedding  $\mathbf{Z}_{all}$ :

$$\mathbf{Z}_{all} = \begin{bmatrix} \mathbf{Z}_p \\ \mathbf{Z}_k \end{bmatrix} \in \mathbb{R}^{(N_p + N_k) \times H}. \quad (9)$$

Then, we propose to apply the L2-norm on the unified embedding  $\mathbf{Z}_{all}$  to ensure it has a comparable scale regardless of the type of entity, analogous to (7), creating  $|\mathbf{Z}_{all}|$ . Finally, we calculate the full score matrix  $\mathbf{S}$  using a scaled dot-product:

$$S = \alpha |\mathbf{Z}_{all}| |\mathbf{Z}_{all}|^T \in \mathbb{R}^{(N_p + N_k) \times (N_p + N_k)}, \quad (10)$$

where  $\alpha$  is the learnable scale parameter learned during training from (8), and  $\mathbf{S}$  has the following block structure:

$$\mathbf{S} = \begin{bmatrix} \mathbf{S}_{pp} & \mathbf{S}_{pk} \\ \mathbf{S}_{kp} & \mathbf{S}_{kk} \end{bmatrix}, \quad \mathbf{S}_{kp} = \mathbf{S}_{pk}^\top. \quad (11)$$

The full score matrix  $\mathbf{S}$  contains similarity scores for both cross-entity interactions between parameters and KPI ( $S_{pk}$ ), as well as same-entity relationships among parameters ( $\mathbf{S}_{pp} \in \mathbb{R}^{N_p \times N_p}$ ) and among KPIs ( $\mathbf{S}_{kk} \in \mathbb{R}^{N_k \times N_k}$ ). While  $\mathbf{S}_{pk}$  is learned from training on measurements between parameters and KPIs, the same-entity blocks  $\mathbf{S}_{pp}$  and  $\mathbf{S}_{kk}$  instead emerge after training by evaluating pairwise alignments among parameters and among KPIs in the shared latent space, respectively.

### V. PROPOSED GRAPH RECONSTRUCTION METHOD

The score matrix  $\mathbf{S}$  provides a soft representation of interactions between entities, capturing information about the behavior and state of the RAN. However, it does not provide the topological information required for identifying conflicts. To accomplish this, we reconstruct a conflict graph by mapping  $\mathbf{S}$  into  $\hat{\mathbf{A}}_{\text{learned}}$  with topological information that encodes potentially conflicting relationships. This requires determining the relevant interactions in  $\mathbf{S}$  that constitute actual relationships, and binarizing them using the indicator function  $\mathbb{1}(\cdot)$  to obtain an adjacency matrix representing a conflict graph.

There are several conventional techniques used in machine learning tasks to determine relevant interactions based on the distribution of score values. These include: (i) selecting a reconstruction threshold  $\tau$  and retaining all score values above it; (ii) selecting a fixed number of  $K$  relevant scores, and retaining the top- $K$  highest score values; or (iii) choosing a representative  $Q$  percentage of the score distribution, and retaining the top  $Q\%$  of scores. However, all these techniques share the same fundamental limitation: they require parameterization and manual fine-tuning on a given score distribution to find appropriate values for  $\tau$ ,  $K$  or  $Q$ . As a result, conflict detection solutions using these methods are difficult to generalize across datasets and deployment scenarios [3], [5].

To address this limitation, we adopt *sparsemax* [11], a data-driven normalization function. Sparsemax maps real-valued scores to a probability distribution by projecting each row of  $\mathbf{S}$  onto the probability simplex via an Euclidean projection, yielding a sparse representation that retains only strong interactions while weaker interactions collapse exactly to zero. As such, sparsemax provides a general and autonomous mechanism for determining relevant interactions that can be applied across datasets and deployment scenarios without manual fine-tuning.

First, we apply the sparsemax operator to  $\mathbf{S}$  as follows:

$$[\mathbf{P}]_{i,:} = \text{sparsemax}([\mathbf{S}]_{i,:}), \quad \forall i = 1, \dots, (N_p + N_k), \quad (12)$$

where  $\mathbf{P} \in [0, 1]^{(N_p + N_k) \times (N_p + N_k)}$  denotes the resulting sparse probability matrix. Since sparsemax inherently collapses all weak interactions to exact zeros, we can retain all relevant interactions by binarizing  $\mathbf{P}$  using a fixed threshold  $\tau_{\text{sparse}} = 0$ , yielding the learned adjacency matrix  $\hat{\mathbf{A}}_{\text{learned}}$ :

$$[\hat{\mathbf{A}}_{\text{learned}}]_{i,j} = \mathbb{1}([\mathbf{P}]_{i,j} > 0), \quad i \neq j. \quad (13)$$

Finally, we augment  $\hat{\mathbf{A}}_{\text{learned}}$  with known information about  $\mathbf{A}_{\text{known}}$ , as defined in (3), yielding the full adjacency

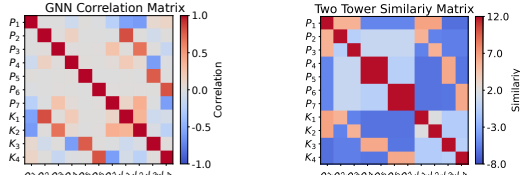


Fig. 3: Example score matrices capturing interactions between parameters and KPIs, highlighting the different metrics and scales associated with correlation (left) and similarity (right).

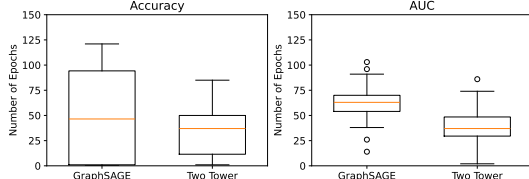


Fig. 4: Classification performance of different models in terms of accuracy and AUC across 100 independent training batches.

matrix  $\hat{A}$  that represents a conflict graph and supports the use of conflict identification methods [5].

## VI. NUMERICAL RESULTS

In this section, we validate our two-tower encoder architecture for interaction learning, and our sparsity-based approach for autonomous conflict graph reconstruction. First, we describe our dataset and training process. Then, we assess the performance of our two towers for learning interactions between parameters and KPIs, and its impact on conflict detection. Next, we assess the performance of sparsemax for reconstructing graphs, and evaluate its impact on conflict detection.

### A. Dataset and Training

To evaluate our proposed two-tower encoder architecture for interaction learning, we adopted a dataset commonly used in the conflict detection literature [5], [8], based on a conflict model for cognitive autonomous networks proposed in [12]. This dataset contains  $L = 10,000$  samples of Gaussian-distributed parameters and KPIs, capturing the evolution of  $N_a = 4$  agents,  $N_p = 7$  parameters, and  $N_k = 4$  KPIs. For information about the structure of the conflict model and how it defines the interactions between agents, parameters, and KPIs, we refer the reader to [5]. To learn the interactions between the entities in our dataset, we designed two separate encoders of parameters and KPIs, each tailored to the corresponding input dimensions. In addition, we used the Adam optimizer with a learning rate of 0.001 [14], with the latent space dimension of  $H = 16$ , which performed the best in our evaluation.

We trained our model using the Binary Cross Entropy (BCE) loss, to minimize the difference between the learned similarities and the ground-truth label matrix  $\mathbf{Y} \in \{0, 1\}^{N_p \times N_k}$ .

The associated loss function is defined as:

$$\mathcal{L}_{\text{BCE}} = \frac{1}{N_p N_k} \sum_{i=1}^{N_p} \sum_{j=1}^{N_k} \ell([S_{pk}]_{i,j}, [\mathbf{Y}]_{i,j}), \quad (14)$$

where  $\ell(\cdot)$  denotes the per-sample loss, given by  $\ell(x, y) = \max(x, 0) - xy + \log(1 + e^{-|x|})$ . After the training, we use the partial score matrix  $S_{pk}$  with learned interactions to reconstruct a complete score matrix  $S$ , as detailed in Section IV-B.

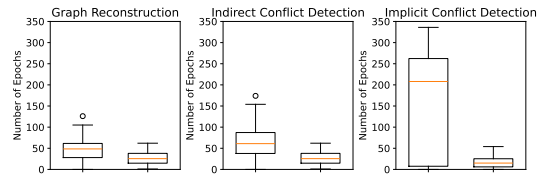


Fig. 5: Graph reconstruction and conflict identification performance using the interactions learned from different models in terms of F1 score across 100 independent training batches.

### B. Two-tower Encoder Learning Performance

In this analysis, we evaluate our two-tower encoder architecture's performance for learning interactions, allowing us to reconstruct conflict graphs and identify conflicts. We compared our two-tower model against the GNN solution proposed in [5]. Fig. 3 presents an instance of the score matrix  $S$  output by the two models after training, where our two-tower model exhibits more distinct separation between classes than the GNN, indicating that similarity is a more discriminative metric for learning interactions than correlation. In Fig. 4, we assess the classification performance of the two models using training accuracy, capturing their ratio of correctly predicted interactions, and Area Under the Curve (AUC), capturing their ability to distinguish existing from non-existing interactions. The GNN requires a median of 47 and 63 training epochs to reach 80% accuracy and AUC, respectively, whereas our model achieves the same performance nearly twice as fast, at a median of 37 epochs for both metrics, due to the more discriminative class separation offered by the similarity scores, which simplifies the training of our two-tower model.

### C. Two-tower Encoder Detection Performance

In this analysis, we assess the performance of the two models to express interactions for enabling the identification of indirect and implicit conflicts, using the F1 score. To this end, we adopted the static threshold for score binarization and rule-based conflict identification approach proposed in [5]. Fig. 5 shows the results of our measurements. The GNN requires a median of 49 epochs to enable the reconstruction of conflict graphs with perfect performance ( $F1 = 1.0$ ), whereas our two-tower model achieves the same twice as fast, at a median of 25 epochs. We can observe a similar behavior for indirect conflict detection, where the GNN requires a median of 61 epochs, while our model reaches the same in 26 epochs. Moreover, the GNN requires a median of 208 epochs to enable perfect detection performance, whereas our two-tower model attains the same after only 15 epochs, yielding nearly a  $14\times$  improvement in training efficiency. This is due to the different learning methods of the two models. Our model directly calculates alignments in the latent space, whereas the GNN progressively propagates information over message-passing iterations, slowing the emergence of complex interactions from implicit conflicts. These results demonstrate that our two-tower encoder architecture is more suited for learning complex interactions than existing GNN-based solutions.

### D. Autonomous Graph Reconstruction Performance

In this analysis, we assess the performance of our proposed data-driven, sparsity-based approach using sparsemax for

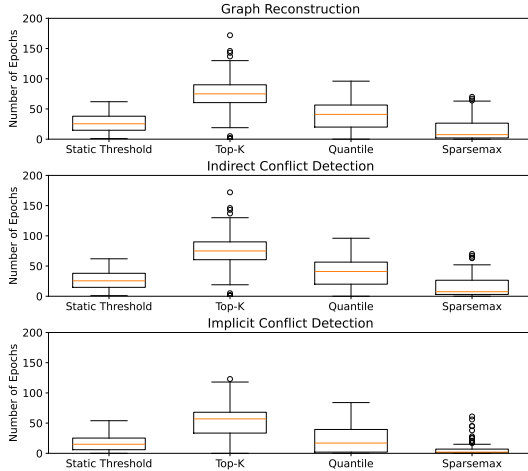


Fig. 6: Comparison of graph reconstruction methods in terms of training efficiency required to achieve perfect performance ( $F1 = 1$ ) for conflict graph reconstruction and conflict identification across 100 independent training batches.

autonomous graph reconstruction. We compared sparsemax against the techniques detailed in Section V, including a static threshold, top- $K$ , and statistical quantiles fine-tuned to our dataset, across 100 independent training batches. For the sake of brevity, we limit our evaluation on the interaction scores output by our two-tower model, which we have shown to offer significant advantages over existing GNN-based solutions.

For graph reconstruction, shown in Fig. 6 (top plot), we observe that the top- $K$  and quantile techniques require substantially stronger interactions resulting from a longer training to achieve perfect reconstruction ( $F1 = 1.0$ ), being  $\approx 2\text{--}3\times$  slower than the static threshold that achieves perfect reconstruction at a median of 26 epochs. In contrast, sparsemax achieves the same at a median of only 8 epochs, yielding a  $4\times$  improvement in training efficiency. This is due to sparsemax’s comparative normalization, which enforces competition among interaction scores, making subtle differences very expressive early in training, enabling faster a faster graph reconstruction.

For conflict detection, we adopted the rule-based identification approach proposed in [5]. We observe a similar trend for indirect conflicts in Fig. 6 (middle plot), where the top- $K$  and quantile techniques are  $\approx 2\text{--}3\times$  slower than the static threshold that achieves perfect identification at a median of 26 epochs, while sparsemax achieves the same at a median of only 15 epochs, yielding  $\approx 2\times$  performance gains. For implicit conflicts, shown in Fig. 6 (bottom plot), the top- $K$  and quantile are  $1\text{--}5\times$  slower than the static threshold at a median of 15 epochs. Meanwhile, sparsemax reaches the same at a median of only 2 epochs, delivering nearly an  $8\times$  performance gains. These results demonstrate that sparsemax is a more effective approach for expressing relevant interactions for graph reconstruction, outperforming other methods while remaining fully autonomous and requiring no manual fine-tuning.

## VII. CONCLUSIONS

In this paper, we introduced a systematic framework for conflict detection in AI-native mobile networks, decomposing the

problem into three stages: interaction learning, graph reconstruction, and conflict identification. We formulated interaction learning as a ranking problem between parameters and KPIs and proposed a lightweight two-tower encoder architecture for efficiently learning these interactions. In addition, we introduced a data-driven, sparsity-based approach for selecting relevant interactions, enabling autonomous conflict graph reconstruction without manual fine-tuning for specific datasets or scenarios. We showed that our proposed solutions outperform state-of-the-art methods across a variety of conflict detection tasks, from conflict graph reconstruction to identification of different types of conflicts. In future works, we plan to investigate temporal models in our two-tower encoders to capture the dynamic evolution of the RAN, and deploy our proposed solutions in a AI-native network environment.

## ACKNOWLEDGEMENTS

Work supported through the INL Laboratory Directed Research & Development (LDRD) Program under DOE Idaho Operations Office Contract DE-AC07-05ID14517. This research was also partially funded by the NSF IUCRC WISPER, under NSF Award Nos. 2412872, 2413009, and 2413168, and by the NSF US-Ireland R&D Partnership program under NSF Award No. 2421362. The research leading to this paper also received support from the Commonwealth Cyber Initiative.

## REFERENCES

- [1] N. A. Khan *et al.*, “AI-RAN in 6G Networks: State-of-the-Art and Challenges,” *IEEE Open Journal of the Communications Society (OJ-COMS)*, vol. 5, pp. 294–311, 2023.
- [2] J. F. Santos *et al.*, “Managing O-RAN Networks: xApp Development from Zero to Hero,” *IEEE Communications Surveys & Tutorials*, 2025.
- [3] P. B. del Prever *et al.*, “Pacifista: Conflict Evaluation And Management In Open Ran,” *IEEE Transactions on Mobile Computing*, 2025.
- [4] O-RAN Alliance, “O-RAN Conflict Mitigation,” O-RAN Alliance, Technical Report O-RAN.WG3.TR.ConfMit-R004-v01.00, Oct. 2024.
- [5] A. Zolghadr *et al.*, “Learning and Reconstructing Conflicts in O-RAN: A Graph Neural Network Approach,” in *IEEE Wireless Communications and Networking Conference (WCNC)*, 2025, pp. 01–06.
- [6] P. Sharma *et al.*, “Towards xApp Conflict Evaluation with Explainable Machine Learning and Causal Inference in O-RAN,” *arXiv preprint arXiv:2510.13031*, 2025.
- [7] Y. Shao *et al.*, “Distributed Graph Neural Network Training: A Survey,” *ACM Computing Surveys*, vol. 56, no. 8, pp. 1–39, 2024.
- [8] A. Wadud *et al.*, “QACM: Qos-aware xApp Conflict Mitigation in Open RAN,” *IEEE Transactions on Green Communications and Networking (TGCN)*, 2024.
- [9] Y. Yan *et al.*, “RankTower: A Synergistic Framework for Enhancing Two-Tower Pre-Ranking Model,” *arXiv preprint arXiv:2407.12385*, 2024.
- [10] X. Li *et al.*, “Inttower: The Next Generation of Two-tower Model for Pre-ranking System,” in *ACM International Conference on Information & Knowledge Management (CIKM)*, 2022, pp. 3292–3301.
- [11] A. Martins *et al.*, “From Softmax to Sparsemax: A Sparse Model of Attention and Multi-label Classification,” in *PMLR International Conference on Machine Learning (ICML)*, 2016, pp. 1614–1623.
- [12] A. Banerjee *et al.*, “Toward Control and Coordination in Cognitive Autonomous Networks,” *IEEE Transactions on Network and Service Management (TNSM)*, vol. 19, no. 1, pp. 49–60, 2021.
- [13] A. Wadud *et al.*, “xApp-level Conflict Mitigation in O-RAN, A Mobility Driven Energy Saving Case,” in *IEEE Conference on Computer Communications Workshops (INFOCOM WKSHPS)*, 2025, pp. 1–6.
- [14] F. Z. Lebib *et al.*, “Two-tower Neural Network for Personalizing Service Recommendation in Cloud Environment,” in *IEEE International Multi-Conference on Systems, Signals & Devices (SSD)*, 2025, pp. 879–884.
- [15] Y. Shen *et al.*, “A Two-tower Spatial-temporal Graph Neural Network for Traffic Speed Prediction,” in *Springer Pacific-Asia Conference on Knowledge Discovery and Data Mining (PAKDD)*, 2022, pp. 406–418.